MITSUBISHI ELECTRIC RESEARCH LABORATORIES
http://www.merl.com

Fading Characterization in a Semi-Anechoic Chamber with Artificial Scatterers for Mean Effective Gain Measurements of Wireless Handheld Terminals

Andres Alayon Glazunov, Andreas Molisch, Fredrik Tufvesson

TR2008-043 August 2008

Abstract

This paper presents the methodology and corresponding analysis of the scattered field measurements in a semianechoic ferrite-lined chamber. The focus is on recreating a Rayleigh fading environment with realistic cross-polarization ratio (XPR) with the purpose of measuring the Mean Effective Gain (MEG) of mobile handheld terminal operating in the 900 MHz GSM band. The emulated XPR was similar in each of the studied scenarios and approximately equal to 12 dB. The Rayleigh fading hypothesis for the statistics of the envelope of the measured signals could not be rejected in most cases at the 955 level with the Kolmogorov goodness-of-fit test.

IEEE Radio and Wireless Symposium

Fading characterization in a semi-anechoic chamber with artificial scatterers for Mean Effective Gain measurements of wireless handheld terminals

Andrés Alayón Glazunov[1], Andreas F. Molisch[1,2] and Fredrik Tufvesson[1]
[1]Dept. of Electrical and Information Technology, Lund University, Box 118, SE-221 00, Lund Sweden
[2]Mitsubishi Electric Research Labs, Cambridge, MA 02139, USA
Email: (Andres.Alayon, Andreas.Molisch, Fredrik.Tufvesson)@eit.lth.se

***Abstract*— This paper presents the methodology and corresponding analysis of the scattered field measurements in a semi-anechoic ferrite-lined chamber. The focus is on recreating a Rayleigh fading environment with realistic cross-polarization ratio (XPR) with the purpose of measuring the Mean Effective Gain (MEG) of mobile handheld terminal operating in the 900 MHz GSM band. The emulated XPR was similar in each of the studied scenarios and approximately equal to 12 dB. The Rayleigh fading hypothesis for the statistics of the envelope of the measured signals could not be rejected in most cases at the 95 % level with the Kolmogorov goodness-of-fit test.**

I. Introduction

The radio communication efficiency of a mobile handheld terminal can have a considerable impact on the capacity and therefore on a more cost effective deployment of cellular wireless networks, [1]. For example, if the mobile antenna efficiency is impaired by high losses, the link quality will worsen considerably leading to poor receiver sensitivity, which in turn affects the capability of the receiver to decode the incoming signals. Moreover, in the uplink a poor antenna efficiency implies that higher input power has to be delivered to the handheld antenna.

The Mean Effective Gain (MEG) [2], [3] is a key quantity to measure the uplink communication performance of mobile handheld terminals. A standard way of measuring MEG is the "Telia scattered field method" described in [4] and [5]. In this method, the power transmitted by the mobile device is compared to the power transmitted by a calibrated dipole antenna. This method allows measuring the communication power of a handheld terminal including the antenna by re-creating real life scenarios in laboratory conditions. The environment emulated is the non line-of-sight (NLOS) scenario, which usually leads to a Rayleigh distributed envelope of the fading signal measured at the handheld terminal. Another important parameter that relates to the propagation environment is the cross-polarization ratio (XPR), i.e., the ratio of the average power of the vertically polarized ($\hat{\theta}-$polarized) waves to the average power of the horizontally polarized ($\hat{\phi}-$polarized) waves incoming at the antenna.

In the past, the antenna test measurements have been performed in not so well controlled scattered field environments, [4], [5]. Our solution is to move the measurement set-up to a shielded ferrite-lined chamber that absorbs electromagnetic signals at frequencies up to 1 GHz. The final goal is to reduce uncertainty sources like errors due to interference and the difficulty to perform measurements with good repeatability due to changes in the environment. In this paper we present a thorough investigation of accuracy of the proposed method in terms of fading statistics and XPR, with good repeatability. The measurements were performed at the 900 MHz GSM band.

II. Chamber propagation measurements

A. Background

We study the envelope of the received signal variation in the shielded chamber at the working frequency in order to control the measurement environment and the error sources. The measured signal is modelled as the sum of the direct path between the antennas and the paths produced by reflections on walls, the floor and ceiling and as in our case some scattering objects such as corrugated metallic sheets. The statistical distribution of the variation of the signal envelope is thus given by the Rice distribution, $p_R(r) = \frac{r}{\sigma} e^{-\frac{r^2+s^2}{2\sigma^2}} I_0\left(\frac{rs}{\sigma^2}\right)$. The Rice distribution is characterized by two parameters, P and K (or σ and s). P is the second moment of the distribution and in our specific application it stands for the average received power, which is computed after removing the distance dependence from the total received power. K is defined as the ratio of the power of the direct (deterministic) component s^2, to the power of the scattered field $2\sigma^2$, i.e., $K = \frac{s^2}{2\sigma^2}$. The total received power in the line-of-sight (LOS) regime P_r, is computed by the Friis transmission formula,

$$P_\mathrm{r}(d,f) = \frac{P_\mathrm{t} G_\mathrm{t} G_\mathrm{r}}{L_\mathrm{c}(f)\, L_0(d,f)}, \tag{1}$$

where P_t is the transmitted power, G_t and G_r are the antenna gains of the transmitting and receiving antennas, respectively, $L_\mathrm{c}(f)$ denotes losses in cables, contacts and losses due polarization mismatch, and $L_0(d,f)$ is the free space path loss usually observed in LOS communication given by $L_0(d,f)_\mathrm{dB} = 32.4 + 20\log\left(f_{[\mathrm{GHz}]}\right) + 20\log\left(d_{[\mathrm{m}]}\right)$, where

d is the distance between the antennas and f is the frequency. In the NLOS regime we assume that no distance dependence is present as shown later in Fig 2. Hence, the power of the "scattered field", expressed in dB, may then be computed as, $2\sigma^2_{\mathrm{dB}} = -L_0\left(d,f\right)_{\mathrm{dB}} - 10\log\left(1+K\right)$, where the path loss and the Ricean K-factor are computed at unit distance in meters.

We estimate the signal attenuation in the chamber in both the vertical and horizontal polarizations by measuring the corresponding path loss. Two calibrated half-wavelength dipoles with baluns are used for this purpose. Fig. 1a) shows a schematic representation of the measurement set-up for the vertical-to-vertical antenna configuration. The small circles with continuous radius represent the horizontal pattern of the vertically polarized half-wavelength dipole antenna. On the other hand, in order to measure the horizontal-to-horizontal attenuation the dipoles are tilted 90° from the vertical. It is well known that the antenna pattern of a dipole is not omnidirectional in this case. However, assuming that the distribution of the incoming waves at the transmitting antenna position (Tx) is uniform in the azimuth and mainly confined to the horizontal plane, a fairly good evaluation of the path loss of the horizontally polarized components is obtained.

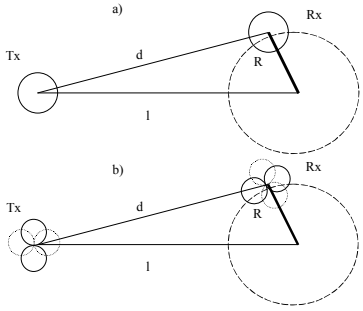

Fig. 1. Schematic representation of the vertical-to-vertical measurements a) and horizontal-to-horizontal measurements b).

Next, we show briefly how to assess the horizontally polarized components. The antenna pattern for the vertically polarized half-wave dipole antenna is constant in the azimuth, on the other hand in elevation it is proportional to $1.64\sin^3\left(\theta\right)$. If the dipole antenna is tilted 90° from the vertical, a good approximation is still the same function but now of the azimuth instead of the elevation angle, [6]. Then, the gain pattern for one horizontal orientation is $G_{\phi 1}\left(\phi\right) \approx 1.64\sin^3\left(\phi\right)$, while for the one perpendicular to it as sketched in Fig.1b) is given by $G_{\phi 2}\left(\phi\right) \approx 1.64\cos^3\left(\phi\right)$. Hence, the total gain is, $G_{\phi}\left(\phi\right) \approx G_{\phi 1}\left(\phi\right) + G_{\phi 2}\left(\phi\right)$. By the superposition principle we can add the particular contributions obtained for the four possible combinations of the horizontal-to-horizontal scenarios as shown in Fig.1 b). The total received power expressed in linear scale may then be computed as, $P_{\mathrm{r}} = P_{90^\circ,0^\circ} + P_{90^\circ,90^\circ} + P_{0^\circ,0^\circ} + P_{0^\circ,90^\circ}$, where the two subindexes denote one of the two possible antenna orientations in the horizontal plane. Further, writing each of the terms accordingly to the Friis equation (1), $P_{\mathrm{r}}\left(d,f\right) = \frac{P_{\mathrm{t}}}{L_c L_0}\left(G_{\mathrm{t},90^\circ}G_{\mathrm{r},0^\circ} + G_{\mathrm{t},90^\circ}G_{\mathrm{r},90^\circ} + G_{\mathrm{t},0^\circ}G_{\mathrm{r},0^\circ} + G_{\mathrm{t},0^\circ}G_{\mathrm{r},90^\circ}\right)$. Finally, in virtue of that the transmitted power, the path loss and cable losses are the same for all measurements, after grouping common terms the following equation is obtained, $P_{\mathrm{r}}\left(d,f\right) = \frac{P_{\mathrm{t}}}{L_c L_0}\left(G_{\mathrm{t},90^\circ} + G_{\mathrm{t},0^\circ}\right)\left(G_{\mathrm{r},90^\circ} + G_{\mathrm{r},0^\circ}\right)$. Thus, after this manipulation the equivalent antenna pattern for both, the transmitting and the receiving antennas $G_{\phi}\left(\phi\right)$ is fairly omnidirectional.

As mentioned earlier, one of our main goals is to emulate realistic values of the XPR of the channel by introducing artificial scatterers in the chamber. As a start we need a shielded chamber with 0 dB polarization imbalance, i.e., a perfect polarization balance achieved at a co-polarization ratio (CPR) equal to the unity, where $CPR = \frac{P_{\mathrm{VV}}}{P_{\mathrm{HH}}}$, P_{VV} is the average power measured between two vertically co-polarized antennas, P_{HH} is the corresponding value for the horizontally polarized antennas. The XPR is defined as, $\chi = \frac{P_{\mathrm{VV}}}{P_{\mathrm{VH}}}$, where P_{VH} is the corresponding value for the cross-polarized antennas and P_{VV} has been defined earlier. It is worthwhile to notice that the link powers involving horizontal polarization should be compensated for the fact that the resulting pattern in the horizontal polarization is not uniform. It can be shown that for the uniform distribution of the power confined to the horizontal plane the corresponding error will be $10\log10(8/3\pi)$, which is equal to $0.7\ dB$. Thus, 0.7 dB and 1.4 dB should be added to the measured P_{VH} and P_{HH}, respectively. It is also worthwhile to notice that if only one of the two orthogonal antenna positions (corresponding to the horizontal polarization) was used, a correction factor of 3 dB should be added to the obtained average signal, [7].

B. Measurements and analysis

In this section we present calibration measurements performed in a semi-anechoic chamber. Reflections in the frequency range up to 1 GHz are attenuated by the ferrite coating placed all over the floor, walls and ceiling of the chamber. The first step of the investigation was therefore to measure the reflections inside the chamber so a controlled emulation of a scattered field could be performed. Besides the reflections produced by the coating material and the measurement equipment inside the chamber, an additional source of reflections was present, namely the metallic door of the chamber that was not covered by the absorbing coating. Absorbing cones on a plank mitigated these reflections.

The propagation measurements were performed at the 900 MHz GSM band, results are shown in Fig. 2. Both, P_{VV} and P_{HH} measurements were carried out according to the method described above. From the P_{VV} measurements the signal variation is due to both imperfections of the chamber and the signals caused by the presence of the measurement equipment have been estimated. In this case, the envelope variation and its average will correctly reflect the propagation and losses in prevailing conditions. On the other hand, from the P_{HH} measurements only the average power may be estimated, since an assessment of the fading statistics would not be correct.

Five different distances l were chosen according to Fig. 1 and three measurement scenarios were considered. The first one was a LOS scenario, i.e., both antennas could see each other. The second and the third were in NLOS where copper wire netting and a copper sheet were used in order to obstruct the direct path between the antennas.

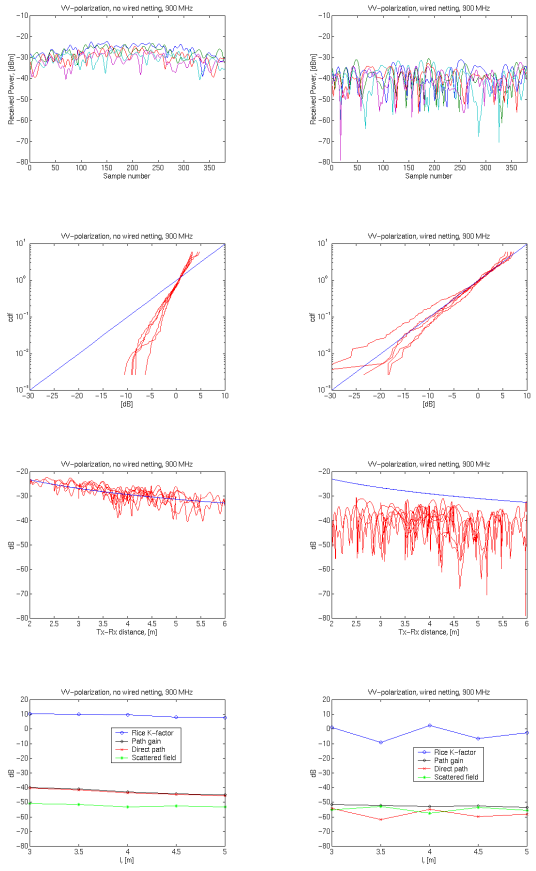

Fig. 2. Measurement results in LOS (left) and NLOS (right) regimes. First raw from the top: measured signal, second raw: envelope statistics in a Rayleigh chart, third raw: path loss dependence and forth raw: K-factor, total-, direct- and scattered field path loss.

The left column of Fig. 2 shows the results for the LOS scenario. As can be seen, there are several sources of reflections that cause the signal variation measured at different distances in the LOS scenario. The amplitude of the signal, as expected, decreases with distance. Certainly, according to Friis equation (1), the power amplitude of the direct path will decrease with distance and therefore approach the amplitude of the power reflected from the scatterers present in the room. Their power also decreases with distance but with slower rate than the direct path. The resulting fading variation can then be characterized by the Rice distribution. The K-factor of the empirical distribution is obtained by the method of moments [8]. It is around 10 dB, which shows that there are still considerable reflections in the chamber. The cdf of the signal envelope is shown on a Rayleigh chart (second plot from the top on the left column of Fig.2). The power imbalance expressed by the CPR is in this case quite near 0 dB as required.

In the NLOS case, when the direct path is absent, the signal variation resembles more the Rayleigh fading (second plot from the top on the right side in Fig.2). In this case, all scattered paths have similar power amplitudes independently of the distance between the antennas. The total average power signal is now of the same magnitude as the scattered field component of the LOS measurements, which is expected. The estimated K-factor varied considerably if expressed in dB, however in most cases it remained below 3 dB, which is a good indication of a Rayleigh distribution, yet not a sufficient condition as it will be shown below.

The Kolmogorov goodness-of-fit test, [9] was used to test envelope statistics. It works by comparing the order statistics of the sample distribution with the theoretical distribution, and testing the largest difference against a theoretically determined difference. In all cases, the largest deviation was near zero. Thus the null hypothesis that the distribution is Rayleigh could not be rejected at the 95 % significance level in most cases. In LOS, the Rayleigh hypothesis was rejected in all cases. On the other hand, the same hypothesis was accepted in most cases in NLOS, except the measurements at 4 m. In those cases, a strong signal component due to reflections could be the reason for the higher K-factor. But also for some measurements obtained at 4.5 m distance with copper netting, the hypothesis was rejected despite the low K-factor. Overall, we can conclude that in most cases the Rayleigh distribution fits data rather well in NLOS scenarios.

III. Emulation of a Scattered Field Environment

The mobile propagation environment is emulated by placing artificial scatterers at different positions in the measurement chamber. In order to obtain different scenarios, metallic plates with square tooth profiles were used. As already explained above, the focus was on obtaining a good Rayleigh environment and on being able to obtain a realistic XPR in the chamber. A more rigorous analysis of the effects of the metallic sheets on the propagation would involve quite complicated scattering theories. However, a simplified yet still accurate analysis may be achieved by applying the Rayleigh criterion [10], which uses the following parameter in order to estimate the roughness of a surface, $C = \frac{4\pi\delta}{\lambda}\sin(\psi)$, where δ is the maximum deviation of the surface, λ is the wavelength and ψ is the grazing angle. Hence, according to the Rayleigh criterion, the surface is smooth for $C < 0.1$, while for $C > 10$ it is considered rough. Setting $\delta = 0.10$ m and $\lambda = 0.33$ m leads to $C = 3.8\sin(\psi)$. This means that the specular reflection and the diffuse component are of similar magnitude for grazing angles larger than $1.5°$, which according to the geometry of the measurement site will be always satisfied. Consequently, both the specular and the diffuse reflection components will be present. The second propagation mechanism that may contribute to the total field is diffraction over the edges of the copper sheet obstructing the LOS between the antennas. It can be shown by using Fresnel diffraction formulas [10], that the power of the diffracted rays

will be at least 10 dB lower than that of an unattenuated LOS component.

In order to maximize the impact of the metallic sheets, they were placed with the longer side perpendicularly to the floor of the chamber. We measured six scenarios, i.e., six different placements of the metallic sheets; the arrangements are shown in Fig. 3. Two distances, 4 and 4.5 m, between the transmitter position and the centre of the circle described by the receiver antenna were chosen for the NLOS scenario with the copper sheet. Measurement results are shown Tables I and II.

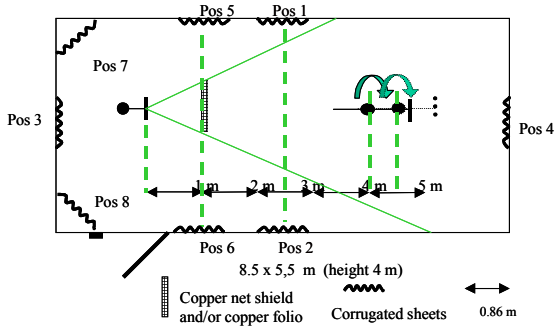

Fig. 3. Sketch of the plate placements. The six scenarios are: I-1,2, II-1,2,3, III-1,2,3,4, IV-1,2,5,6, V-1,2,3,5,6, VI-3,5,6,7,8

As can be seen from the tables, there was no significant difference between those two distances in terms of the measured envelope statistics or the measured XPR, which remained almost constant with a span of only 1.5 dB between the maximum and minimum values for all the six scenarios described in Table I. The major impact of the sheets was on the fading statistics, which resulted in regulating the amount of reflections as can be inferred from Table. II. Some of the measurements were repeated several times (the numeric superscript denotes the measurement number) in order to verify the method for repeatability. The agreement was quite good most of the times. The best results were obtained for scenario VI (see Fig. 3 and Table. I and II), which passed the Kolmogorov goodness-of-fit test (the rejected samples were denoted with superscript R) all four times at 4 m and three times at 4.5 m. Furthermore, measurements were performed at the same distances as in the previous section but for scenarios IV and VI. In those scenarios, the metallic sheets were placed closer to the transmitter, which should emulate a uniform power distribution around the transmitter in a better way than the other arrangements. Even here, the XPR changed only slightly. The statistics remained Rayleigh in most cases.

IV. Conclusions

Based on the results presented above we can conclude that scattered field measurements are feasible in semi-anechoic shielded chambers by placing objects that act as scatterers inside the chamber. Both the fading statistics and cross-polarization ratio of real propagation scenarios may be reproduced. However, further investigations are required to fully evaluate the potential of this method for the assessment of the communication performance of mobile handheld terminals in controlled propagation environments.

TABLE I

Rice K-factor for the VV antenna configurations for the six measurement scenarios according to Fig.3 and at l=4, 4.5 m

	K_{VV}						
l, [m]	4.0				4.5		
I	0.9^{1}		$0.9^{3,R}$		0.8^{1}		
II	0.6^{1}		$2.7^{3,R}$		0.7^{1}		
III	0.6^{1}		$1.4^{3,R}$		0.8^{1}		
IV	0.4^{1}	0.2^{2}	0.6^{3}	$0.2^{4,R}$	0.6^{1}	0.6^{2}	$1.2^{4,R}$
V	$0.5^{1,R}$		$0.8^{3,R}$		0.2^{1}		
VI	1.0^{1}	0.7^{2}	0.9^{3}	0.7^{4}	0.2^{1}	0.4^{2}	0.1^{4}

TABLE II

XPR and CPR for the six measurement scenarios measured at l=4 m and 4.5 m, according to Fig.3

	XPR, [dB]			CPR, [dB]			
l, [m]	4.0		4.5	4.0		4.5	
I	12.2^{3}		-	0.2^{1}		-0.9^{1}	
II	12.2^{3}		-	-0.4^{1}		-1.2^{1}	
III	11.8^{3}		-	-0.1^{1}		-0.5^{1}	
IV	12.7^{3}	12.3^{3}	11.8^{4}	0.6^{1}	1.5^{2}	-0.6^{1}	-1.1^{2}
V	13.1^{3}			0.3^{1}		-1.2^{1}	
VI	13.2^{3}	12.2^{4}	12.2^{4}	-2.1^{1}	-1.4^{2}	-1.9^{1}	-2.1^{2}

Acknowledgments

Part of this work was supported by TeliaSonera Sweden, SSF High Speed Wireless Center and an INGVAR grant from the Swedish Foundation for Strategic Research.

References

[1] A. Alayon Glazunov, "Joint impact of the mean effective gain and base station smart antennas on wcdma-fdd systems performance," in *Nordic Radio Symposium, Oulu, Finland*, 2004.

[2] T. Taga, "Analysis for mean effective gain of mobile antennas in land mobile radio environments," *Vehicular Technology, IEEE Transactions on*, vol. 39, pp. 117–131, May 1990.

[3] A. Alayon Glazunov, A. F. Molisch, and F. Tufvesson, "On mean effective gain of antennas," *Antennas and Propagation, IEEE Transactions on*, 2007. (submitted).

[4] B. G. H. Olsson and S. Å. Larsson, "Description of antenna test method performed in scattered field environment for gsm ms," in *COST259WG2.2*, 1998.

[5] M. Knudsen, G. Pedersen, B. Olsson, K. Olesen, and S.-A. Larsson, "Validation of handset antenna test methods," in *Vehicular Technology Conference, 2000. IEEE VTS-Fall VTC 2000. 52nd*, vol. 4, pp. 1669–1676vol.4, 24-28 Sept. 2000.

[6] A. C. Balanis, *Antenna Theory: Analysis and Design*. Wiley, 1997.

[7] D. Cox, R. Murray, H. Arnold, A. Norris, and M. Wazowicz, "Cross-polarization coupling measured for 800 mhz radio transmission in and around houses and large buildings," *Antennas and Propagation, IEEE Transactions on [legacy, pre - 1988]*, vol. 34, pp. 83–87, Jan 1986.

[8] L. J. Greenstein, D. G. Michelson, and V. Erceg, "Moment-method estimation of the Ricean K-factor," *IEEE Communications Letters*, vol. 3, pp. 175–176, June 1999.

[9] A. Papoulis, *Probability, Random Variables and Stochastic Processes*. No. ISBN 0-07-048477-5 in International Edition, Mc Graw-Hill International Edition, 1991.

[10] R. Vaughan and J. B. Andersen, *Channels, propagation and antennas for mobile communications*. IEE, 1 ed., 2003.